Catalytic Function of the Conserved Hydroxyl Group in the Protein Tyrosine Phosphatase Signature Motif†

Zhong-Yin Zhang,*,‡ Bruce A. Palfey,§ Li Wu,‡ and Yu Zhao‡

Department of Molecular Pharmacology, Albert Einstein College of Medicine, Bronx, New York 10461, and Department of Biological Chemistry, The University of Michigan, Ann Arbor, Michigan 48109

Received August 9, 1995; Revised Manuscript Received October 16, 1995⊗

ABSTRACT: Burst kinetics is observed with the *Yersinia* protein tyrosine phosphatase (PTPase). This provides direct kinetic evidence for a phosphoenzyme mechanism and suggests that the breakdown of the phosphoenzyme intermediate is the rate-limiting step. Burst kinetics is a powerful tool for mechanistic studies of PTPase catalysis since functional roles of active site residues can be evaluated by studying their effects on the individual elementary steps associated with the formation and the breakdown of the intermediate. In order to investigate the role of Thr410, a conserved residue that is present in the PTPase signature motif, this residue was altered by site-directed mutagenesis to serine and alanine. The effects of these mutations, as observed in both steady-state and pre-steady-state kinetic experiments with *p*-nitrophenyl phosphate (*p*NPP) as a substrate, demonstrated that the hydroxyl group of Thr410 is directly involved in catalysis. The hydroxyl group at residue 410 plays an important role in facilitating the breakdown of the phosphoenzyme intermediate.

Protein tyrosine phosphatases (PTPases) are signaling molecules that act in concert with protein tyrosine kinases to regulate a variety of fundamental cellular processes including cell growth and proliferation, cell cycle control, and cytoskeletal integrity (Walton & Dixon, 1993). The PTPases constitute a family of enzymes (now >40 members) that rival the protein tyrosine kinases in terms of structural diversity and complexity. The PTPases can be categorized into two groups: receptor-like and intracellular PTPases. The unique feature that defines the PTPase family is the active site sequence (H/V)**C**(X)$_5$**R**(S/T) in the catalytic domain called the PTPase signature motif (Zhang, Z.-Y., et al., 1994a) (Figure 1). In addition to the PTPases, there exist two additional groups of phosphatases, the VH1-like dual-specificity phosphatases and the low molecular weight phosphatases, which can utilize substrates containing phosphotyrosine as well as phosphoserine/threonine (Guan et al., 1991; Zhang et al., 1995). Interestingly, the VH1-like dual-specificity phosphatases, the low molecular weight phosphatases, and the tyrosine-specific PTPases share the active site motif (H/V)**C**(X)$_5$**R**(S/T) (Figure 1) but display little amino acid sequence identity outside of the active site. The invariant Cys residue has been shown to be essential for PTPase activity and formation of a covalent phosphoenzyme intermediate (Guan & Dixon, 1991; Wo et al., 1992; Cho et al., 1992; Cirri et al., 1993; Zhou et al., 1994). The invariant Arg residue in the signature motif plays an important role in substrate binding and transition-state stabilization (Zhang, Z.-Y., et al., 1994a).

Phosphatase	Sequence
Yop51	V I H **C** R A G V G **R** **T** A
PTP1B	V V H **C** S A G I G **R** **S** G
CD45	V V H **C** S A G V G **R** **T** G
VH1	L V H **C** A A G V N **R** **S** G
VHR	L V H **C** R E G Y S **R** **S** P
PAC-1	L V H **C** Q A G I S **R** **S** A
Low Mr. PTP	L F V **C** L G N I C **R** **S** P
human cdc25	F V H **C** E F S S E **R** G P

FIGURE 1: PTPase signature motif. The active site sequence alignments of Yop51 (*Yersinia* PTPase) (Michiels & Cornelis, 1988), PTP1B (Chernoff et al., 1990), CD45 (Trowbridge et al., 1991), VH1 (Guan et al., 1991), VHR (Ishibashi et al., 1992), PAC-1 (Rohan et al., 1993), low M_r phosphatase (Wo et al., 1992), and human cdc25 (Gautier et al., 1991).

Recently, the crystal structures of the mammalian PTP1B (Barford et al., 1994) and the *Yersinia* PTPase (Stuckey et al., 1994) have been determined. In addition, the structure of a low molecular weight phosphatase from bovine liver (Su et al., 1994) and bovine heart (Zhang, M., et al., 1994) has also been solved. Although the amino acid sequence of the *Yersinia* PTPase is only ~20% identical to that of PTP1B, it is clear that the two structures share a common secondary structural scaffold, with close similarity in tertiary structure. The low molecular weight phosphatases are unrelated in sequence to the PTPases and have distinct topologies (Su et al., 1994; Zhang, M., et al., 1994). Interestingly, residues of the PTPase signature motif (residues 403−410 in the *Yersinia* PTPase, 214−222 in PTP1B, and 12−19 in the low molecular weight phosphatase) form a similar loop structure termed the phosphate-binding loop between the β-turn at the COOH-terminus of a β strand and the first turn of an α helix (Stuckey et al., 1994; Barford et al., 1994; Su et al., 1994; Zhang, M., et al., 1994). The PTPases and the low molecular

† This work was supported in part by a grant from the National Institutes of Health, DRTC 5P60 DK20541-17 to Z.-Y.Z. B.A.P. was supported by United States Public Health Service Grants to David P. Ballou (GM 20877) and Vincent Massey (GM 11106).

* Correspondence should be addressed to this author. Tel.: (718) 430-4288. FAX: (718) 430-8922.

‡ Albert Einstein College of Medicine.

§ The University of Michigan.

⊗ Abstract published in *Advance ACS Abstracts,* December 1, 1995.

0006-2960/95/0434-16389$09.00/0

weight phosphatases appear to represent striking examples of convergent evolution.

The PTPase−WO_4^{2-} complexes (Stuckey et al., 1994; Barford et al., 1994) reveal that the S atom of Cys403 in the *Yersinia* PTPase is poised 3.6 Å from the W atom while the S atom of Cys215 in PTP1B is poised 3.1 Å from the W atom. Thus, the sulfur atom is in a position for a direct S_N2 nucleophilic attack on a substrate's phosphorus atom. This is consistent with its role as a nucleophile in the catalytic mechanism. The structures of the PTPase−tungstate complexes also show that the tungstate oxygen atom(s) ion pair(s) with the positively-charged Arg409 and Arg221 of the *Yersinia* PTPase and PTP1B, respectively. Thus, the side chain of R409 acts together with the amides of the phosphate-binding loop to bind the substrate and stabilize the transition state.

In this paper, we present a pre-steady-state kinetic analysis of the *Yersinia* PTPase-catalyzed hydrolysis of *p*-nitrophenyl phosphate (*p*NPP). This approach combined with site-directed mutagenesis permits the evaluation of specific contributions of active site amino acid side chains to the individual steps of the PTPase catalysis. As part of the phosphate-binding loop, a conserved Ser or Thr can be found immediately after the invariant Arg residue in almost all PTPases. The dual-specificity phosphatase Cdc25 is the only exception that lacks a hydroxyl group at this position (Figure 1). Interestingly, Cdc25 is several orders of magnitude less reactive than other PTPases (Dumphy & Kumagai, 1991; Zhang et al., 1992). In the *Yersinia* PTPase, the hydroxyl group of the conserved Thr (T410) is the closest proton donor to the active site (C403) thiolate (Stuckey et al., 1994). We show here that the hydroxyl group at Thr410 in the *Yersinia* PTPase plays a critical role in the breakdown of the phosphoenzyme intermediate.

EXPERIMENTAL PROCEDURES

Materials. *p*-Nitrophenyl phosphate (*p*NPP) was from Fluka. Mutagenesis kits were from Bio-Rad. All other chemicals were purchased from Sigma.

Site-Directed Mutagenesis. Substitutions at residue Thr410 of the *Yersinia* PTPase were made by site-directed mutagenesis according to the procedure of Kunkel et al. (1987). The oligonucleotide primers used for the desired substitutions were as follows: T410S, TGGCCGTA*G*TGCGCAACTG; T410A, TTGGCCGT*GC*TGCGCAACT; and T410V, GTGTTGGCCGT*GT*TGCGCAACTG. All of the mutations were verified by DNA sequencing (Sanger et al., 1977).

Expression and Purification of the Recombinant Enzymes. The wild type *Yersinia* PTPase and mutants T410S and T410A were expressed in *Escherichia coli* and purified to homogeneity as described (Zhang et al., 1992). In the case of T410V, the recombinant protein was produced as inclusion bodies when expressed in *E. coli*.

Steady-State Kinetics. All enzyme assays were performed in buffers with a constant ionic strength of 0.15 M. Buffers used were as follows: pH 3.8−5.7, 100 mM acetate; pH 5.8−6.5, 50 mM succinate; pH 6.6−7.3, 50 mM 3,3-dimethylglutarate; and pH 7.5−9.0, 100 mM Tris. All of the buffer systems contained 1 mM EDTA, and the ionic strength of the solutions was kept at 0.15 M using NaCl. Initial rate measurements for the enzyme-catalyzed hydrolysis of aryl phosphate monoesters were conducted as previously described (Zhang et al., 1992). The Michaelis−Menten

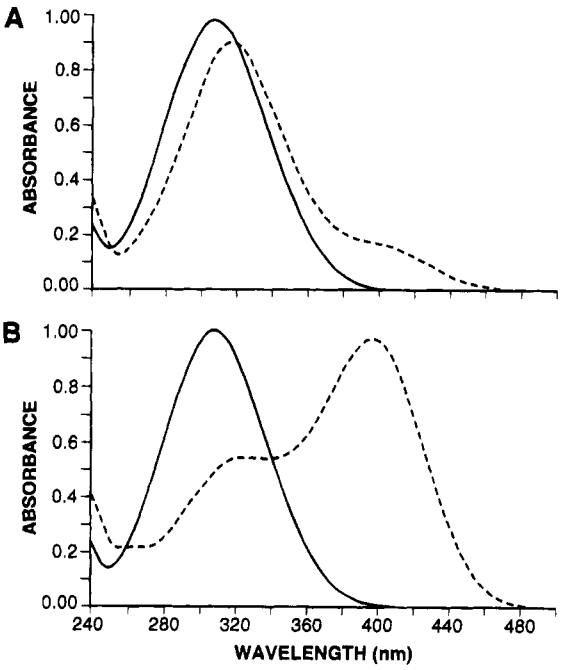

FIGURE 2: Absorption spectra for *p*NPP (solid line) and *p*-nitrophenol (dashed line) at pH 6 (A) and 7.2 (B). Both *p*NPP and *p*NP concentrations were 0.1 mM.

kinetic parameters were determined from a direct fit of the v vs [S] data to the Michaelis−Menten equation using the nonlinear regression program GraFit (Erithacus Software). pH dependence data were fitted to the appropriate equations using a nonlinear least-squares regression program (KaleidaGraph, Synergy Software). Inhibition constants for the *Yersinia* PTPases by inorganic phosphate and arsenate were determined as previously described (Zhang, Z.-Y., et al., 1994a). All experiments were performed in triplicate.

Pre-Steady-State Kinetics. Pre-steady-state kinetic measurements of the *Yersinia* PTPase- and its Thr410 mutant-catalyzed hydrolysis of *p*NPP were conducted using a Hi-Tech SF-61 stopped-flow spectrophotometer (dead time, 2 ms) with an observation cell length of 1.0 cm. Fast reactions at 3.5 °C were monitored by the increase in absorbance at 410 nm of the *p*-nitrophenolate product. The extinction coefficient for *p*-nitrophenolate at 3.5 °C is 985 M^{-1} cm^{-1} at pH 5.8, 1486 M^{-1} cm^{-1} at pH 6.0, and 8914 M^{-1} cm^{-1} at pH 7.2 (Figure 2). The enzyme concentration (determined from the absorption at 280 nm using the value of $A_{280}^{1\%} = 0.352$ and a molecular weight of 51 000) were 9.85−60 μM for the wild type enzyme, 12−53 μM for T410A, and 29.9 μM for T410S. The buffers used were as described above. Data were collected on a Macintosh computer interfaced to the Hi-Tech stopped-flow spectrophotometer using the program KISS (Kinetic Instruments, Inc.). Each stopped-flow trace was an average of at least six individual experiments. The specific rate constants were analyzed by fitting the experimental data directly to the theoretical equation through the use of the nonlinear least-squares algorithm in KISS. The analysis of burst kinetics has been described previously (Bender et al., 1967). Briefly, when [S] ≫ [E], the increase in *p*-nitrophenolate concentration as a function of time can be described as [*p*-nitrophenolate] = $At + B(1 - e^{-bt})$. When the experiments are performed at saturating concentrations of substrate, the individual rate constants for the enzyme phosphorylation (k_2) and dephosphorylation (k_3)

Scheme 1

$$E + ROPO_3^{2-} \underset{k_{-1}}{\overset{k_1}{\rightleftharpoons}} E \cdot ROPO_3^{2-} \xrightarrow{k_2} E\text{-}P \xrightarrow{k_3} E + P_i$$

ROH

can be determined from the exponential ($b = k_2 + k_3$) and the linear [$A = k_2k_3/(k_2 + k_3)$] phases, respectively (Scheme 1). The size of the burst, B equals $E_o[k_2/(k_2 + k_3)]^2/(1 + K_m/S_o)^2$ and is proportional to the active enzyme concentration. For the burst amplitude equivalent to the number of functioning active sites [E_o], the ratio of k_2/k_3 must be very large as must the ratio of S_o/K_m.

Kinetics and pH Dependence of Iodoacetate Inactivation of T410A. The experimental procedures for following the inactivation of the T410A mutant and the analysis of the pH dependence of the inactivation rate for the determination of the active site thiol pK_a were the same as described earlier (Zhang & Dixon, 1993).

RESULTS

To evaluate the role of T410 in PTPase catalysis, it was changed (a) to serine, the lower homolog with the hydroxyl group retained, (b) to alanine, which lacks both the methyl and the hydroxyl groups of the threonine side chain, and (c) to valine, which is isosteric with threonine but lacks hydrogen-bonding capacity. There should be minimal functional alterations in the T410S mutant, since it represents a conservative change at this position and since either Thr or Ser residue can be found at this position in other PTPases [Cdc25 proteins are the only exceptions and possess either a Gly or an Ala residue at this position instead (Figure 1)]. Unfortunately, the valine substitution at 410 resulted in inclusion bodies when expressed in *E. coli* and was therefore not pursued further. Both T410A and T410S mutants were purified to homogeneity and characterized in detail, and both mutants were found to have chromatographic and spectral characteristics similar to those of the wild type, suggesting that there were no major changes in the structure of the mutants. In addition, a number of kinetic properties are shared between the wild type enzyme and mutants T410S and T410A, indicating that no major alteration in structure is due to these substitutions.

The pK_a of the Active Site Cysteine in the T410A Mutant Yersinia PTPase. It has been shown previously that the alkylating agent, iodoacetate, irreversibly inactivates PTPases (Pot & Dixon, 1992; Zhang & Dixon, 1993). The covalent attachment of iodoacetate was specific to the active site cysteine residue. Thus, the apparent pK_a of the active site thiol can be determined from the pH dependency of iodoacetate modification of the *Yersinia* PTPase. The apparent pK_a of the active site Cys403 thiol group in T410A is 5.26 ± 0.09 (Figure 3), which is 0.59 pK unit higher than that of the wild type enzyme (4.67 ± 0.15; Zhang & Dixon, 1993). The second-order rate constant (k_2^{lim}) for the inactivation of T410A is 222 ± 11 M^{-1} min^{-1}, which is 3.7-fold faster than that of the wild type enzyme (59.7 ± 1.3 M^{-1} min^{-1}; Zhang & Dixon, 1993), consistent with the notion that the nucleophilicity of a nucleophile increases as its pK_a is raised.

Steady-State Kinetic Analysis of the Thr410 Mutant Yersinia PTPases. The competitive inhibition constants for the binding of inorganic phosphate by T410A and by the wild type enzyme were determined to be 0.62 ± 0.1 mM and 6.1 ± 0.3 mM, respectively, at pH 6.0. Using arsenate as an inhibitor, the competitive inhibition constant was 1100 ± 70 μM for the wild type enzyme, 390 ± 10 μM for T410S, and 13 ± 0.4 μM for T410A at pH 6.0. Thus, elimination of the hydroxyl group at 410 enhances the binding affinity for inorganic phosphate and arsenate by 10- and 85-fold respectively. The kinetic parameters of the *Yersinia* PTPase and its Thr410 mutants at three different pH values (pH 5, 6, and 7) and 30 °C using *p*NPP as a substrate are listed in Table 1. Serine substitution for threonine at 410 has minimal effect on the kinetic parameters, with about a 2-fold decrease in k_{cat} and nearly identical k_{cat}/K_m values when compared with the wild type enzyme. The kinetic parameters of T410A mutant, however, showed different pH dependencies when compared to those of the wild type. Thus, at pH 5.0, T410A exhibited k_{cat} and k_{cat}/K_m values that are 65- and 8.3-fold lower, respectively, than those of the wild type enzyme. They are 21- and 3-fold lower than the wild type enzyme at pH 6.0 and approach those of the wild type enzyme at pH 7.0.

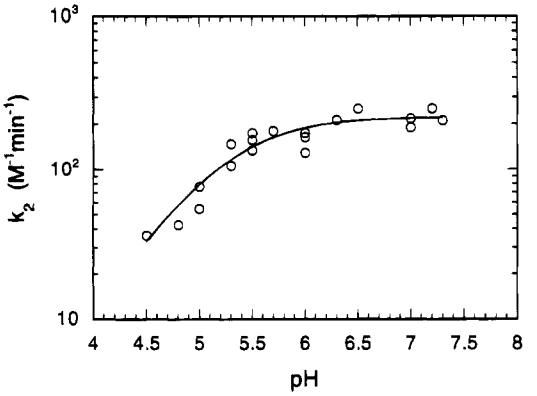

FIGURE 3: pH dependence of the inactivation of the mutant *Yersinia* PTPase T410A by iodoacetate. Reaction conditions were specified under Experimental Procedures. The line in the figure was obtained by a direct fit of the data to equation $k_2 = k_2^o/(1 + [H^+]/K_a)$, where k_2^o is the pH independent inactivation rate constant and K_a is the acid dissociation constant. This equation was employed for calculation of the pK_a value.

Table 1: Summary of Kinetic Parameters of the *Yersinia* PTPase and Its T410 Mutants Using *p*NPP as a Substrate at 30 °C

	pH 5.0		pH 6.0		pH 7.0	
PTPase	k_{cat} (s^{-1})	k_{cat}/K_m (mM^{-1} s^{-1})	k_{cat} (s^{-1})	k_{cat}/K_m (mM^{-1} s^{-1})	k_{cat} (s^{-1})	k_{cat}/K_m (mM^{-1} s^{-1})
wild type	1200	400	335	129	30.2	12.9
T410S	529	264	116	151	19.4	19.8
T410A	18.3	48.2	15.8	43.6	12.4	11.9

Detailed pH dependencies of the kinetic parameters of the T410A and T410S were investigated. For the analysis of k_{cat}/K_m, eq 1 was used, where $(k_{cat}/K_m)^{lim}$ was the pH

$$\frac{k_{cat}}{K_m} = \frac{\left(\frac{k_{cat}}{K_m}\right)^{lim}}{\left(1 + \frac{H}{K_{S2}}\right)\left(1 + \frac{H}{K_{E1}} + \frac{K_{E2}}{H}\right)} \quad (1)$$

independent second-order rate constant, K_{S2} the second ionization constant of the substrate, and K_{E1} and K_{E2} the ionization constants of the free enzyme (Zhang, Z.-Y., et al., 1994b). As expected, the kinetic parameters of T410S behave in a nearly identical manner to those of the wild type

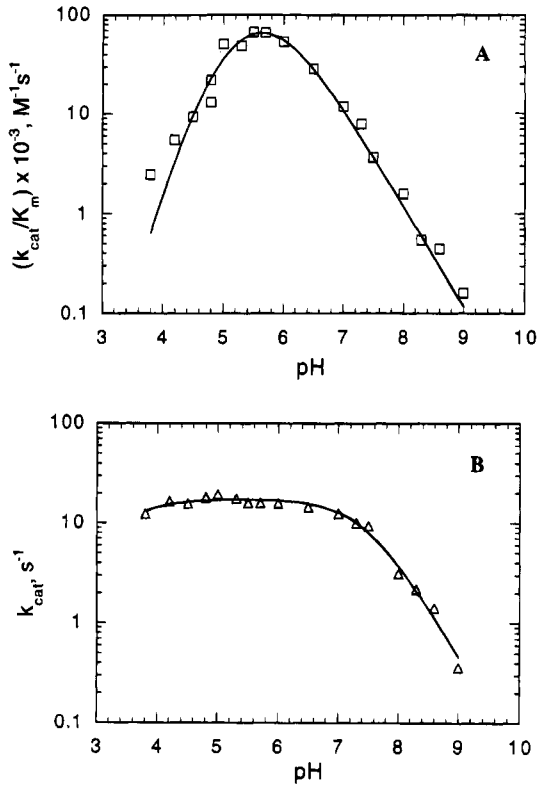

FIGURE 4: A, Effect of pH on k_{cat}/K_m for the mutant *Yersinia* PTPase T410A-catalyzed hydrolysis of *p*NPP (□). The line that is drawn through the experimental data is based on the nonlinear least-squares fit of the data to eq 1. B, Effect of pH on k_{cat} for the mutant *Yersinia* PTPase T410A-catalyzed hydrolysis of *p*NPP (△). The line that is drawn through the experimental data is based on the nonlinear least-squares fit of the data to eq 2.

Table 2: Kinetic Parameters for the *Yersinia* PTPase-Catalyzed Hydrolysis of *p*NPP at 30 °C

PTPase	pK_{E1}	pK_{E2}	$(k_{cat}/K_m)^{lim} \times 10^{-4}$ M^{-1} s^{-1}
wild type[a]	3.28 ± 0.19	5.10 ± 0.16	118 ± 42
T410A	4.76 ± 0.22	5.93 ± 0.14	13.9 ± 2.3

PTPase	pK_1^{app}	pK_2^{app}	k_{cat}^{lim}, s^{-1}
wild type[a]	4.63 ± 0.07	5.20 ± 0.06	2114 ± 250
T410A	3.30 ± 0.15	7.43 ± 0.07	17.6 ± 0.44

[a] Values for the wild type enzyme are taken from Zhang, Z.-Y., et al. (1994b) and are included for comparison.

enzyme (data not shown). The variation of the kinetic parameters of the T410A mutant PTPase-catalyzed hydrolysis of *p*NPP as a function of pH was analyzed (Figure 4) and compared with those of the wild type enzyme (Table 2). Like the wild type enzyme, the variation of k_{cat}/K_m with pH yielded a bell-shaped curve with limiting slopes of +2 on the acid side and −1 on the alkaline side (Figure 4A), suggesting that two groups must be unprotonated and one group must be protonated for activity. The $pK_{S2} = 5.1$ corresponds to the second ionization of *p*NPP, which must be in the dianionic form for optimal catalysis (Zhang, Z.-Y., et al., 1994b). It was shown from the pH dependence of k_{cat}/K_m that the wild type *Yersinia* PTPase requires an ionizing residue that must be deprotonated with a pK_{E1} value of 3.3 and another ionizing residue that must be protonated with a pK_{E2} value of 5.1 for optimal binding and catalysis. For the T410A mutant, pK_{E1} is 4.8 and pK_{E2} is 5.9, 1.5, and 0.8 p*K* units higher that those of the wild type enzyme (Table 2). The pH independent apparent second-order rate constant $(k_{cat}/K_m)^{lim}$ for T410A is 8.5-fold lower than that of the wild type enzyme.

The most dramatic effect of the Thr410 to Ala mutation is manifested in the pH−k_{cat} profile (Figure 4B). For the analysis of k_{cat}, eq 2 was used, where k_{cat}^{lim} is the pH

$$k_{cat} = \frac{k_{cat}^{lim}}{1 + \frac{H}{K_1^{app}} + \frac{K_2^{app}}{H}} \quad (2)$$

independent turnover number and K_1^{app} and K_2^{app} are the apparent ionization constants of the enzyme−substrate complex. When *p*NPP was used as a substrate, pK_1^{app} and pK_2^{app} were 4.6 and 5.2, respectively, for the wild type enzyme (Zhang, Z.-Y., et al., 1994b). Due to the closeness of the two apparent ionization constants in the pH−k_{cat} profile of the wild type *Yersinia* PTPase, a plateau was never reached. In contrast, a clear plateau is observed between pH 4.2 and 6.5 in the pH−k_{cat} profile of the T410A mutant using *p*NPP as a substrate (Figure 4B). The apparent ionization constants, pK_1^{app}, and pK_2^{app} are 3.3 and 7.4 for the T410A substrate complex, respectively. Thus, pK_1^{app} and pK_2^{app} are pushed outward by 1.3 and 2.2 p*K* units, respectively, compared with those of the wild type enzyme (Table 2). Moreover, the pH independent maximum turnover number k_{cat}^{lim} for the T410A mutant is decreased by 120-fold.

Burst Kinetics of the Yersinia PTPases and Effect of Substitutions at Residue Thr410. Since PTPase catalysis involves a covalent phosphoenzyme intermediate, the catalyzed reaction must be composed of at least two chemical steps, *i.e.*, formation and breakdown of the phosphoenzyme intermediate. The phosphoryl group is first transferred to the nucleophilic active site thiolate group of the enzyme to form the phosphoenzyme intermediate, which is then hydrolyzed by water (Scheme 1). The kinetic scheme is composed of substrate binding, followed by two chemical steps, phosphorylation (k_2) and dephosphorylation (k_3), where E is the enzyme, $ROPO_3^{2-}$ the substrate, E·$ROPO_3^{2-}$) the enzyme−substrate Michaelis complex, E−P the phosphoenzyme intermediate, ROH the phenol, and P_i inorganic phosphate. If the net rate of intermediate breakdown is slower than that of intermediate formation, one would predict a "burst" of *p*-nitrophenol production using *p*NPP as a substrate. Attempts to observe such a burst were unsuccessful at room temperature. The turnover number of the *Yersinia* PTPase reaches 1200 s^{-1} at 30 °C (Zhang et al., 1992), which is at the detection limit of a stopped-flow spectrophotometer (dead time 1−2 ms). When the *Yersinia* PTPase-catalyzed hydrolysis of *p*NPP was monitored at 3.5 °C and 410 nm (to detect the *p*-nitrophenolate ion product) using a relatively high concentration of enzyme (10−50 μM), the absorbance time course was biphasic, characterized by a rapid, exponential increase followed by a slower linear increase (Figure 5). Similar observations have been made for a number of well-known hydrolytic enzymes, including α-chymotrypsin (Bender et al., 1967) and elastase (Bender & Marshall, 1968), for which catalysis involves rate-limiting breakdown of a covalent acyl−enzyme intermediate.

By varying the initial concentration of the enzyme and the substrate (Figure 6) we found that the burst is proportional

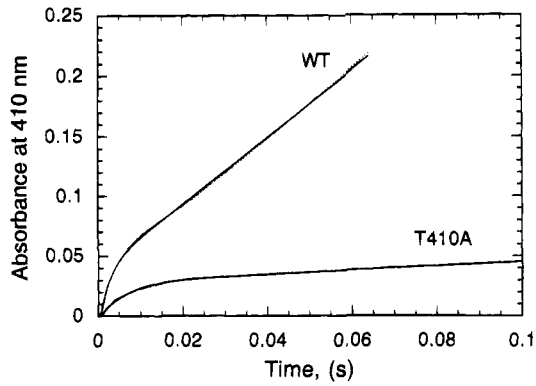

FIGURE 5: Burst kinetics observed with the wild type and T410A mutant *Yersinia* PTPase and *p*NPP at pH 6 and 3.5 °C. The wild type enzyme concentration was 41.4 μM, and T410A concentration was 45 μM. The *p*NPP concentration was 20 and 4 mM for the wild type and T410A *Yersinia* PTPase, respectively. Each stopped-flow trace was an average of at least six individual experiments. The solid line represents a theoretical fit of the data to the equation [*p*-nitrophenolate] = $At + B(1 - e^{-bt})$.

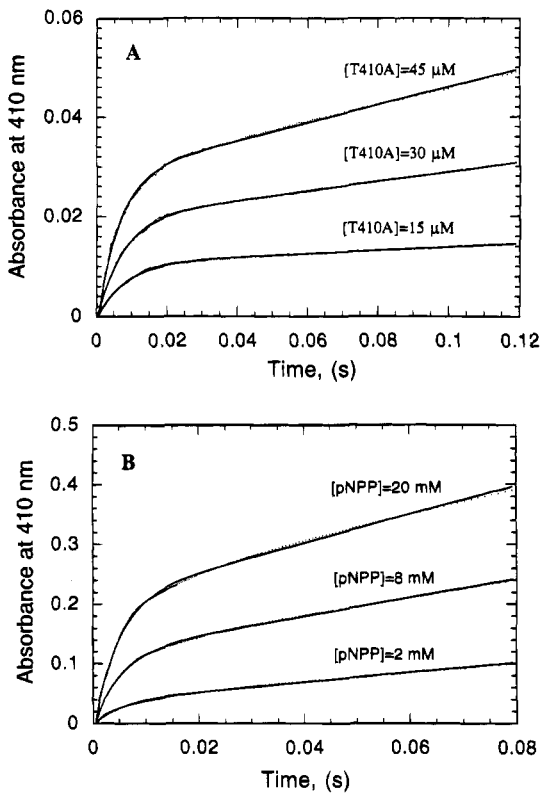

FIGURE 6: Effects of enzyme concentration (A) and substrate concentration (B) on the burst magnitude. A, T410A mutant *Yersinia* PTPase and 4 mM *p*NPP at pH 6. B, 39.4 μM wild type *Yersinia* PTPase and *p*NPP at pH 7.2. Each stopped-flow trace was an average of at least six individual experiments. The solid line represented a theoretical fit of the data to the equation [*p*-nitrophenolate] = $At + B(1 - e^{-bt})$.

to the enzyme concentration and that the dependency of the burst size on the substrate concentration can be adequately described by $B = E_o[k_2/(k_2 + k_3)]^2/(1 + K_m/S_o)^2$. In general, the observed amplitudes of bursts for the wild type enzyme agree fairly well with the theoretical values calculated using the above equation. The bursts for the T410A mutant at pH 6.0 were 55−60% of the analytical enzyme concentration, whereas the calculated theoretical value was 76%, based on 4 mM *p*NPP, K_m being 0.5 mM and k_2 and k_3 being 144 and 2.6 s^{-1}, respectively. Thus, the experimentally determined bursts for T410A mutant only amounted to 72%−80% of the theoretical values. It is possible that the T410A preparation was only 80% active, which then gave rise to the slightly less than stoichiometric bursts observed.

Although the pH optimum for the *Yersinia* PTPase-catalyzed hydrolysis of *p*NPP is around 5 (Zhang, Z.-Y., et al., 1994b), we conducted our stopped-flow measurements at pH 5.8, 6.0, and 7.2, since only the *p*-nitrophenolate anion is chromogenic (the pK_a of the *p*-nitrophenol is 7.14) (Figure 2). Table 3 lists the steady-state kinetic parameters determined independently of the stopped-flow experiments at 3.5 °C for the wild type and the T410A mutant *Yersinia* PTPase at pH 5.8, 6.0, and 7.2. Table 4 summarizes the individual rate constants for the formation and decay of the phosphoenzyme intermediate for the wild type and the T410A mutant PTPase under the same conditions. Each set of the rate constants (k_2 and k_3) were determined directly from the average of at least six to eight individual stopped-flow traces. The rate constant for the phosphoenzyme intermediate formation, k_2, is relatively insensitive to variation of pH from 5.8 to 7.2 for both the wild type *Yersinia* PTPase and the T410A mutant. The rate constant for the breakdown of the intermediate, k_3, is nearly identical to the k_{cat} value determined from steady-state experiments under the same conditions. The pH dependencies of k_3 for both the wild type and the T410A mutant also resemble those of the k_{cat}. This is in accord with k_3 and k_{cat} representing the same chemical step, *i.e.*, the breakdown of the phosphoenzyme intermediate. It appears that the elimination of the hydroxyl group at Thr410 has only a modest effect on k_2 (a 2-fold reduction), whereas its major impact seems to be primarily reflected in k_3, especially at low pH values. Figure 5 shows the differential effects of Ala substitution at residue 410 on k_2 and k_3 at pH 6.0 (also see Table 4). The effect on k_3 changes with pH, causing a different k_{cat}−pH profile from the wild type enzyme (shown above). Thus, with T410A, k_3 is slowed down by 30-fold at pH 5.8, 19-fold at pH 6.0, and 2.7-fold at pH 7.2. Serine substitution for threonine at residue 410 (T401S) causes only a 1.7- and 1.6-fold decrease in k_2 and k_3, respectively, at pH 7.2 (data not shown).

DISCUSSION

The apparent pK_a of the active site thiol in the *Yersinia* PTPase is 4.67 (Zhang & Dixon, 1993), which is nearly 4 pK_a units lower than the pK_a of a Cys residue in proteins (Lundblad & Noyes, 1984). A reduction in the pK_a of this magnitude for a thiol requires unusual stabilization by its surrounding residues. Unlike the cysteine proteinases, which stabilize an active site thiolate anion *via* an ion-pair with a protonated histidine (Lewis et al., 1981), the PTPases stabilize the active site thiolate by an extensive network of H-bonds radiating from the phosphate-binding loop (Barford et al., 1994; Stuckey et al., 1994). In the *Yersinia* PTPase structure, the Cys403 S is located between 3.0 and 4.2 Å from every amide nitrogen of the phosphate-binding loop, making reasonable S−HN hydrogen bonds (Gregoret et al., 1991) for effective thiolate anion stabilization. In particular, it is observed that the closest proton donor to the thiolate anion is the hydroxyl group of Thr410 which corresponds to a hydrogen-bonding distance of 2.8 Å (Stuckey et al., 1994). The finding that elimination of the hydroxyl group at position 410 elevated the apparent active site thiol pK_a by 0.59 pK unit is consistent with the fact that it plays a

Table 3: Summary of Steady-State Kinetic Parameters of the *Yersinia* PTPase and Its T410A Mutant Using *p*NPP as a Substrate at 3.5 °C

	pH 5.8		pH 6.0		pH 7.2	
PTPase	k_{cat} (s^{-1})	K_m (mM)	k_{cat} (s^{-1})	K_m (mM)	k_{cat} (s^{-1})	K_m (mM)
wild type	68.9 ± 9.6	2.80 ± 0.6	45.6 ± 2.2	2.30 ± 0.12	7.70 ± 0.19	2.50 ± 0.16
T410A	3.15 ± 0.09	0.81 ± 0.021	2.86 ± 0.11	0.50 ± 0.06	2.86 ± 0.27	1.54 ± 0.13

Table 4: Rate Constants for the Formation (k_2) and the Breakdown (k_3) of the Phosphoenzyme Intermediate of the *Yersinia* PTPase and Its T410A Mutant Using *p*NPP as a Substrate at 3.5 °C[a]

	pH 5.8		pH 6.0		pH 7.2	
PTPase	k_2	k_3	k_2	k_3	k_2	k_3
wild type	343	76	346	49	193	6.5
T410A	140	2.5	144	2.6	97	2.4

[a] All values in s^{-1}.

Scheme 2: Thermodynamic Relationship between the Ionized and Unionized Active Site Thiol in the Wild Type Enzyme and in the T410A Mutant[a]

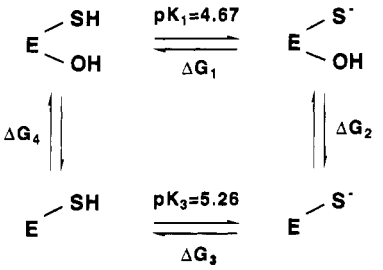

[a] Legend: E, *Yersinia* PTPase; SH, thiol group of the active site Cys403; OH, hydroxyl group of Thr410.

role in stabilizing the thiolate anion. The thermodynamic scheme shown below (Scheme 2) describes the energetics associated with the elimination of a hydroxyl group at Thr410, $\Delta\Delta G = \Delta G_2 - \Delta G_4 = \Delta G_3 - \Delta G_1 = 2.303RT(pK_1 - pK_3) = -0.80$ kcal/mol. Thus, the hydrogen bond strength between the Thr410 hydroxyl and the Cys403 thiolate is 0.8 kcal/mol stronger than the corresponding hydroxyl and thiol interaction. In other words, the hydroxyl side chain of Thr410 interacts preferentially with the thiolate anion to enhance its stability. It is important to point out that the hydroxyl group of Thr410 alone certainly does not account for all of the thiolate stabilization, as evidenced by the still-low pK_a of the thiol in the T410A mutant. The backbone amide hydrogen bonds from the phosphate-binding loop (Stuckey et al., 1994) and the side chain of His402 (Zhang & Dixon, 1993) also contribute to this stabilization.

It has been argued that an enzyme can utilize a portion of the intrinsic enzyme−substrate binding energy to increase the overall rate of a reaction (Jencks, 1975). In such mode of catalysis, the enzyme makes use of the binding energy to juxtapose substrate and enzyme active site functional groups that would not otherwise interact in the ground state but that do interact strongly in the transition state. The observed weaker binding of phosphate by the wild type *Yersinia* PTPase relative to the T410A mutant suggests that the introduction of a hydroxyl group at position 410 (wild type enzyme) destabilizes the ground-state interaction. Thus, the excess binding energy observed in the T410A mutant is sacrified by the wild type enzyme in order to increase the value of k_{cat}. The net outcome is that k_{cat}/K_m for T410A drops by only several-fold while a more pronounced decrease is observed for k_{cat}. A similar example of an amino acid side chain involved in ground-state destabilization is Lys258 in aspartate aminotransferase (Toney & Kirsch, 1993).

Our burst kinetic results are most consistent with the phosphoenzyme mechanism, in which the breakdown of the phosphoenzyme intermediate is the rate-limiting step. Supporting evidence includes the facts that up to 27%−74% of PTPase can be trapped as a covalent adduct using ^{32}P-labeled substrate (Guan & Dixon, 1991; Wo et al., 1992) and that such an intermediate can be prepared in sufficient amount for ^{31}P NMR analysis (Wo et al., 1992; Cho et al., 1992). Interestingly, burst kinetics was also observed with the low molecular weight phosphatase (Zhang & Van Etten, 1991) and the mammalian PTPase, PTP1 (Zhang, 1995). In both cases, the burst kinetics was interpreted by a phosphoenzyme mechanism that involves a rate-limiting breakdown of the intermediate.

In view of the kinetic consequences of the Thr410 to Ala mutation, we propose that the most important role for Thr410 is to stabilize the transition state of the dephosphorylation step facilitating the breakdown of the phosphoenzyme intermediate. Under pre-steady-state conditions at 3.5 °C, where rate constants for the individual elementary steps can be directly measured, we demonstrated that the elimination of the hydroxyl group at residue 410 decreases k_2, the phosphorylation rate, by only 2-fold, whereas up to a 30-fold reduction in k_3, the dephosphorylation rate, is observed at pH 5.8. That the hydroxyl group of Thr410 effectively facilitates catalysis in the rate-limiting breakdown of the phosphoenzyme intermediate is also consistent with steady-state kinetic results. The elimination of the hydroxyl group (T410A) only has a modest influence on k_{cat}/K_m, which probes steps in the mechanism up to the first irreversible step, phosphorylation and release of *p*-nitrophenol, with a 8.5-fold reduction in the pH independent value (Table 2). In contrast, a 120-fold reduction in the pH independent value of k_{cat}, which most likely measures the dephosphorylation (k_3), was observed for the mutant T410A at 30 °C (Table 2).

There is much evidence to indicate that in non-enzyme-catalyzed solution reaction, phosphate monoesters hydrolyze *via* a dissociative mechanism (Butcher & Westheimer, 1955; Bunton et al., 1967; Kirby & Varvoglis, 1967; Gorenstein et al., 1977) involving an unsymmetrically "exploded" metaphosphate-like transition state in which bond formation to the incoming nucleophile is minimal and bond breaking between phosphorus and the leaving group is substantial (Bourne & Williams, 1984; Skoog & Jencks, 1984; Herschlag & Jencks, 1989; Cleland, 1990; Hengge et al., 1994). Recently, we have shown by measuring the heavy-atom kinetic isotope effects associated with the *Yersinia* PTPase and the mammalian PTP1-catalyzed hydrolysis of *p*NPP, that P−O bond cleavage is rate-limiting for the k_{cat}/K_m portion of the mechanism of both enzymes and that the transition state is similar for both enzymes, highly dissociative, and similar to that in solution (Hengge et al., 1995). As a result

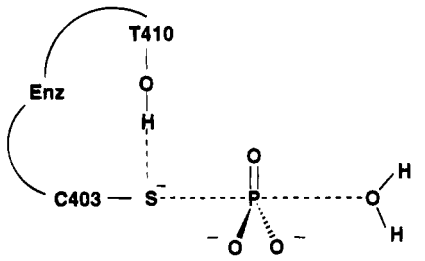

FIGURE 7: A proposed role for the hydroxyl group in the PTPase signature motif during the hydrolysis of the thiophosphate enzyme intermediate in the transition state. The numbers refer to the residues in the *Yersinia* PTPase.

there is a corresponding negative charge developing on the departing phenolic oxygen atom which can be stabilized by protonation. Stabilization of the buildup of the negative charge on the leaving group is one of the potential mechanisms for stabilization of a dissociative transition state (Herschlag & Jencks, 1990). Thus, in the chemical step that leads to the phosphoenzyme formation, the departure of the phenol leaving group is facilitated by the general acid Asp356 (Zhang, Z.-Y., et al., 1994c; Hengge et al., 1995). Nonenzymatic hydrolysis of phosphate monoesters proceeds most facilely at pH 4, where the predominate form corresponds to the monoanion. Hydrolysis of the phosphate monoester monoanions displays a small β_{lg} (−0.27 to −0.32), which is in accord with the departure of a neutral leaving group (Kirby & Varvoglis, 1967; Bunton et al., 1967). These data have been interpreted to imply a pre-equilibrium proton transfer to the bridge oxygen atom followed by phosphorus−oxygen (P−O) bond fission in the rate-limiting step. For leaving groups with $pK_a < 7$, this proton transfer may become rate-limiting (Kirby & Varvoglis, 1967). For thiophosphate monoesters, proton transfer to the bridge sulfur atom throughout the pK_a range 3−12 may become rate-limiting (Milstien & Fife, 1967). A similar need for charge stabilization on the sulfur atom during the hydrolysis of the thiophosphate enzyme intermediate may be required.

The exact mechanism by which Thr410 accelerates the dephosphorylation step is not clear. Both structural (Stuckey et al., 1994) and biochemical data described in this paper suggest that the hydroxyl group of Thr410 interacts with the sulfur atom of the active site nucleophile Cys403. One possibility is that in the step that leads to the hydrolysis of the intermediate the developing negative charge on the thiolate leaving group in the transition state is stabilized by the hydroxyl group at position 410. Figure 7 is depicted with the hydroxyl group of Thr410 hydrogen bonded to the thiolate anion of Cys403 in the transition state of the hydrolysis of the thiophosphate enzyme intermediate. If we assume that the transition state for the hydrolysis of the thiophosphate intermediate is similar to that of the phosphorylation step, *i.e.*, highly dissociative in nature, then charge stabilization on the leaving thiolate will be important since P−S bond breaking is substantial in the transition state. In essence, the hydroxyl group at 410 provides the driving force for the enzyme to go through a dissociative pathway. The loss of such an interaction would make the phosphocysteine more resistant to breakdown. On the other hand, in the transition state that leads to the phosphoenzyme formation, there is little bond making between the nucleophilc thiolate and the phosphorus atom. Thus, it is understandable that elimination of the hydroxyl group at position 410 has a minimal effect on the phosphorylation step because little nucleophilic activation is needed for the reaction.

The structure of the phosphate-binding loop and the invariant Cys and Arg residues in the *Yersinia* PTPase, PTP1B and the low molecular weight phosphatase have been conserved from bacteria to mammals (Barford et al., 1994; Stuckey et al., 1994; Su et al., 1994; Zhang, M., et al., 1994). It is likely that PTPases, dual-specific phosphatases, and low molecular weight phosphatases utilize a similar structural feature, the phosphate-binding loop, within their active sites and employ a common strategy for phosphate monoester hydrolysis. The common catalytic strategy involves the Cys residue acting as the nucleophile to attack the phosphate ester, forming a thiophosphate intermediate, and the invariant Arg residue playing a role both in substrate recognition and transition state stabilization. As part of the phosphate-binding loop, the conserved Thr/Ser residue immediately following the invariant Arg residue facilitates the breakdown of the phosphoenzyme intermediate. Such a role has also been proposed for a dual-specificity phosphatase, VHR (Denu & Dixon, 1995).

ACKNOWLEDGMENT

We thank David Ballou and John Blanchard for the use of their stopped-flow instruments. We also thank Jack Dixon for useful comments on this work.

REFERENCES

Barford, D., Flint, A. J., & Tonks, N. K. (1994) *Science 263*, 1397−1404.
Bender, M. L., & Marshall, T. H. (1968) *J. Am. Chem. Soc. 90*, 201−207.
Bender, M. L., Kezdy, F. J., & Wedler, F. L. (1967) *J. Chem. Educ. 44*, 84−88.
Bourne, N., & Williams, A. (1984) *J. Am. Chem. Soc. 106*, 7591−7596.
Bunton, C. A., Fendler, E. L., Humeres, E., & Yang, K.-U. (1967) *J. Org. Chem. 32*, 2806−2811.
Butcher, W. W., & Westheimer, F. H. (1955) *J. Am. Chem. Soc. 77*, 2420−2424.
Chernoff, J, Schievella, A. R., Jost, C. A., Erikson, R. L., & Neel, B. G. (1990) *Proc. Natl. Acad. Sci. U.S.A. 87*, 2735−2739.
Cho, H., Krishnaraj, R., Kitas, E., Bannwarth, W., Walsh, C. T., & Anderson, K. S. (1992) *J. Am. Chem. Soc. 114*, 7296−7298.
Cirri, P., Chiarugi, P., Camici, G., Manao, G., Raugei, G., Cappugi, G., & Ramponi, G. (1993) *Eur. J. Biochem. 214*, 647−657.
Cleland, W. W. (1990) *FASEB J. 4*, 2899−2905.
Denu, J. M., & Dixon, J. E. (1995) *Proc. Natl. Acad. Sci. U.S.A. 92*, 5910−5914.
Dumphy, W. G., & Kumagai, A. (1991) *Cell 67*, 189−196.
Gautier, J., Soloman, M. J., Booher, R. N., Bazan, J. F., & Kirschner, M. W. (1991) *Cell 67*, 197−211.
Gorenstein, D. G., Lee, Y.-G., & Kar, D. (1977) *J. Am. Chem. Soc. 99*, 2264−2267.
Gregoret, L. M., Rader, S. D., Fletterick, R. J., & Cohen, F. E. (1991) *Proteins 8*, 99−107.
Guan, K. L., & Dixon, J. E. (1991) *J. Biol. Chem. 266*, 17026−17030.
Guan, K. L., Broyles, S., & Dixon, J. E. (1991) *Nature 350*, 359−361.
Hengge, A. C., Edens, W. A., & Elsing, H. (1994) *J. Am. Chem. Soc. 116*, 5045−5049.
Hengge, A. C., Sowa, G., Wu, L., & Zhang, Z.-Y. (1995) *Biochemistry 34*, 13982−13987.
Herschlag, D., & Jencks, W. P. (1989) *J. Am. Chem. Soc. 111*, 7579−7586.
Herschlag, D., & Jencks, W. P. (1990) *Biochemistry 29*, 5172−5179.

Ishibashi, T., Bottaro, D. P., Chan, A., Miki, T., & Aaronson, S. A. (1992) *Proc. Natl. Acad. Sci. U.S.A. 89*, 12170−12174.
Jencks, W. P. (1975) *Adv. Enzymol. Relat. Areas Mol. Biol. 43*, 219−410.
Kirby, A. J., & Varvoglis, A. G. (1967) *J. Am. Chem. Soc. 89*, 415−423.
Kunkel, T. A., Roberts, J. D., & Zakour, R. A. (1987) *Methods Enzymol. 154*, 367−382.
Lewis, S. D., Johnson, F. A., & Shafer, J. A. (1981) *Biochemistry 20*, 48−51.
Lundblad, R. L., & Noyes, C. M. (1984) in *Chemical Reagents for Protein Modification*, Vol. 1, p 56, CRC Press, Boca Raton, FL.
Michiels, T., & Cornelis, G. (1988) *Microb. Pathog. 5*, 449−459.
Milstien, S., & Fife, T. H. (1967) *J. Am. Chem. Soc. 89*, 5820−5826.
Pot, D. A., & Dixon, J. E (1992) *J. Biol. Chem. 267*, 140−143.
Rohan, P. J., Davis, P., Moskaluk, C. A., Kearns, M., Krutzsch, H., Siebenlist, V., & Kelly, K. (1993) *Science 259*, 1763−1766.
Sanger, F., Nicklen, S., & Coulson, A. R. (1977) *Proc. Natl. Acad. Sci. U.S.A. 74*, 5463−5467.
Skoog, M. T., & Jencks, W. P. (1984) *J. Am. Chem. Soc. 106*, 7597−7606.
Stuckey, J. A., Fauman, E. B., Schubert, H. L., Zhang, Z.-Y., Dixon, J. E., & Saper, M. A. (1994) *Nature 370*, 571−575.
Su, X.-D., Taddel, N., Stefani, M., Ramponi, G., & Nordlund, P. (1994) *Nature 370*, 575−578.
Toney, M. D., & Kirsch, J. F. (1993) *Biochemistry, 32*, 1471−1479.
Trowbridge, I. S., Ostergaard, H. L., & Johnson, P. (1991) *Biochim. Biophys. Acta 1095*, 46−56.
Walton, K. M., & Dixon, J. E. (1993) *Annu. Rev. Biochem. 62*, 101−120.
Wo, Y.-Y. P., Zhou, M.-M., Stevis, P., Davis, J. P., Zhang, Z.-Y., & Van Etten, R. L. (1992) *Biochemistry 31*, 1712−1721.
Zhang, M., Van Etten, R. L., & Stauffacher, C. V. (1994) *Biochemistry 33*, 11097−11105.
Zhang, Z.-Y. (1995) *J. Biol. Chem. 270*, 11199−11204.
Zhang, Z.-Y., & Dixon, J. E. (1993) *Biochemistry 32*, 9340−9345.
Zhang, Z.-Y., & Van Etten, R. L. (1991) *J. Biol. Chem. 266*, 1516−1525.
Zhang, Z.-Y., Clemens, J. C., Schubert, H L., Stuckey, J. A., Fischer, M. W. F., Hume, D. M., Saper, M A., & Dixon, J. E. (1992) *J. Biol. Chem. 267*, 23759−23766.
Zhang, Z.-Y., Wang, Y., Wu, L., Fauman, E. B., Stuckey, J. A., Schubert, H. L., Saper, M. A. & Dixon, J. E. (1994a) *Biochemistry 33*, 15266−15270.
Zhang, Z.-Y., Malachowski, W. P., Van Etten, R. L., & Dixon, J. E. (1994b) *J. Biol. Chem. 269*, 8140−8145.
Zhang, Z.-Y., Wang, Y., & Dixon, J. E. (1994c) *Proc. Natl. Acad. Sci. U.S.A. 91*, 1624−1627.
Zhang, Z.-Y., Zhou, G., Denu, J. M., Wu, L., Tang, X., Mondesert, O., Russell, P., Butch, E., & Guan, K.-L. (1995) *Biochemistry 34*, 10560−10568.
Zhou, G., Denu, J. M., Wu, L., & Dixon, J. E. (1994) *J. Biol. Chem. 269*, 28084−28090.

BI951847O